

# Multiple-Electrode Radiofrequency Ablation Creates Confluent Areas of Necrosis: In Vivo Porcine Liver Results<sup>1</sup>

Paul F. Laeseke, BS  
 Lisa A. Sampson, CVT  
 Dieter Haemmerich, PhD  
 Christopher L. Brace, PhD  
 Jason P. Fine, ScD  
 Tina M. Frey, RT(R)  
 Thomas C. Winter III, MD  
 Fred T. Lee, Jr, MD

## Purpose:

To prospectively evaluate, in vivo in pigs, an impedance-based multiple-electrode radiofrequency (RF) ablation system for creation of confluent areas of hepatic coagulation.

## Materials and Methods:

The study was preapproved by the institutional research animal care and use committee. A prototype multiple-electrode RF system that enables switching between three electrically independent electrodes at impedance spikes was created. Forty-two coagulation zones (18 with single, 12 with cluster, and 12 with multiple [three single electrodes spaced 2 cm apart] electrodes) were created at laparotomy in 15 female pigs. Half the ablations were performed for 12 minutes, and half were performed for 16 minutes. The coagulation zones were excised and sliced into approximately 3-mm sections for measurement. Analysis of variance and two-sample *t* tests (with Bonferroni correction,  $\alpha = .0033$ ) were used to assess for differences between groups.

## Results:

At 12 minutes, the mean multiple-electrode coagulation was significantly larger than the mean single-electrode coagulation (minimum diameter, 2.8 vs 1.6 cm; maximum diameter, 4.2 vs 2.0 cm; volume, 22.1 vs 6.7 cm<sup>3</sup>;  $P < .0033$  for all comparisons). The mean maximum diameter achieved at 12 minutes with multiple electrodes was significantly larger than that achieved with the cluster electrode (4.2 vs 2.9 cm,  $P = .02$ ). At 16 minutes, the mean multiple-electrode coagulation (minimum diameter, 3.2 cm; maximum diameter, 4.2 cm; volume, 29.1 cm<sup>3</sup>) was significantly larger than the mean single-electrode (minimum diameter, 1.7 cm; maximum diameter, 2.2 cm; volume, 7.1 cm<sup>3</sup>;  $P < .0033$  for all comparisons) and cluster-electrode (minimum diameter: 2.3 cm,  $P = .007$ ; maximum diameter: 3.2 cm,  $P = .005$ ; volume: 13.1 cm<sup>3</sup>,  $P = .001$ ) coagulations.

## Conclusion:

Compared with the single and cluster systems used as controls, the multiple-electrode RF ablation system enabled the creation of significantly larger coagulation zones.

© RSNA, 2006

<sup>1</sup> From the Departments of Radiology (P.F.L., L.A.S., C.L.B., T.M.F., T.C.W., F.T.L.) and Biostatistics and Medical Informatics (J.P.F.), University of Wisconsin, Box 3252, Clinical Science Center-E3, 600 Highland Ave, Madison, WI 53792; and Department of Pediatrics, Medical University of South Carolina, Charleston, SC (D.H.). Received July 29, 2005; revision requested October 4; revision received December 5; accepted January 10, 2006; final version accepted February 1. Supported in part by Valleylab, Boulder, Colo. **Address correspondence to P.F.L.** (e-mail: [plaeseke@wisc.edu](mailto:plaeseke@wisc.edu)).

**R**adiofrequency (RF) ablation has been used successfully in the treatment of tumors of the liver, lung, bone, breast, and kidney (1–4). Successful tumor ablation is predicated on the complete eradication of the target tumor, as well as an ablative margin, similar in concept to the surgical removal of a tumor plus a surgical margin of approximately 1 cm (5,6). RF ablation has been shown to be highly effective in achieving complete coagulation in tumors smaller than 3.0 cm in diameter (7). However, treatment of larger tumors has been more problematic, with malignancies larger than 4.0 cm in diameter associated with high rates of local tumor progression (8–10).

Several factors have contributed to the inability to consistently achieve complete destruction of large tumors plus an adequate ablative margin. Most important is the fact that current monopolar RF ablation systems are not compatible with simultaneous use of multiple electrodes because of the electrical interactions that occur when electrodes are spaced close together (11–13). Therefore, sequential overlapping ablations are needed to treat all but the smallest tumors (14). Producing a conglomerate zone of coagulation by overlapping multiple sequential ablations is a complex and time-consuming procedure. Microbubbles created by boiling tissue, bleeding, and edema make it difficult to visualize both the tumor and the zone of ablation with either computed tomographic or ultrasonographic guidance (15,16). Furthermore, prolonged treatment times may increase the overall cost, as well as the anesthesia-related complications associated with the ablation procedure (17,18).

Haemmerich et al (13) previously showed ex vivo that by rapidly switching between multiple closely spaced electrodes, one can create large zones of

coagulation. The multiple-electrode system that they used was designed to take advantage of the thermal synergy that is inherent when multiple independent electrodes are placed in close proximity to one another (19). Although encouraging, the experiments used to assess these systems were limited in two ways: An ex vivo model was used, and switching of the electrodes occurred at fixed time intervals. An ex vivo model lacks perfusion, a clinically important factor in electrode performance, and switching the electrodes at fixed time intervals neither accounts for the biologic changes that occur during the ablation nor is time efficient. Thus, the purpose of our study was to prospectively evaluate, in an in vivo porcine model, an impedance-based multiple-electrode RF ablation system for creation of confluent areas of hepatic coagulation.

### Materials and Methods

Financial support and the prototype multiple-electrode RF ablation system used for this project were provided by Valleylab (Boulder, Colo). Two authors (F.T.L., D.H.) have part ownership of the patent covering this system and are consultants for Valleylab. The authors who are not consultants for Valleylab had control over the inclusion of data and information that might have represented a conflict of interest for the two authors who are consultants.

### Animals, Anesthesia, and Procedures

Fifteen large (mean weight, approximately 90 kg) female domestic swine (Arlington Farms, Arlington, Wis) were used for our study. The study was pre-approved by the research animal care and use committee of the University of Wisconsin, and all husbandry and experimental studies were compliant with guidelines for the care and use of laboratory animals (20). Anesthesia was induced with intramuscular tiletamine hydrochloride plus zolazepam hydrochloride (Telazol; Fort Dodge Animal Health, Fort Dodge, Iowa), atropine sulfate (Phoenix Pharmaceutical, St Joseph, Mo), and xylazine hydrochloride (Xyla-Ject; Phoenix Pharmaceutical).

The animals were intubated, and anesthesia was maintained with inhaled isoflurane (Phoenix Pharmaceutical). The liver was surgically exposed by using a chevron incision. RF ablations were performed by using various electrode types (described later in Experimental Groups section).

Pigs have four relatively flat liver lobes—the left lateral, right lateral, left medial, and right medial lobes—and a maximum of one ablation was performed per lobe, with the ablation order varied in each liver. In an effort to prevent lobe size from limiting the larger ablations, we performed multiple- and cluster-electrode ablations in the larger, more vascular medial lobes of the liver, alternating these procedures between the two lobes. Single ablations were performed in one of the smaller lateral lobes of the liver. Several livers were large enough to perform single-electrode ablations in both the lateral lobes and thereby have a larger number of test samples for this group.

After all ablations were performed, the animals were euthanized with an intravenous overdose of pentobarbital sodium plus phenytoin sodium (Beuthanasia-D; Schering-Plough, Kenilworth, NJ) and the livers were removed en bloc. All animals survived the procedures until they were sacrificed. No apparent complications from any of the RF procedures occurred in any ablation group. The multiple-electrode device

### Advance in Knowledge

- In vivo demonstration of thermal synergy and creation of large conglomerate areas of hepatic coagulation are possible with multiple-electrode radiofrequency ablation.

### Published online before print

10.1148/radiol.2411051271

Radiology 2006; 241:116–124

### Abbreviation:

RF = radiofrequency

### Author contributions:

Guarantors of integrity of entire study, P.F.L., L.A.S., C.L.B., F.T.L.; study concepts/study design or data acquisition or data analysis/interpretation, all authors; manuscript drafting or manuscript revision for important intellectual content, all authors; manuscript final version approval, all authors; literature research, P.F.L., L.A.S., D.H., F.T.L.; experimental studies, P.F.L., L.A.S., D.H., C.L.B., T.M.F., T.C.W., F.T.L.; statistical analysis, P.F.L., L.A.S., J.P.F., F.T.L.; and manuscript editing, all authors

See Materials and Methods for pertinent disclosures.

functioned without unexpected events or complications.

### Experimental Groups

Forty-two coagulation zones were created during our study. Groups 1 and 2—the control ablation groups—consisted of ablations performed with a commercially available single-applicator RF ablation system (Cool-tip RF System; Valleylab) that has either a single RF electrode or one multiple-prong cluster RF electrode. In group 1, 18 ablations were performed with the single electrode, while in group 2, 12 ablations were performed with the cluster electrode. In group 3, 12 ablations were performed with a prototype multiple-electrode RF device. A clinical device based on this prototype (Cool-tip Switching Controller; Valleylab) has just become commercially available.

**Control RF ablation groups.**—All of the control RF ablation procedures described in our study were performed by one author (P.F.L., with 2 years experience in preclinical RF ablation) with the single-applicator Cool-tip system. The RF generator is a 480-kHz monopolar generator that operates at a maximum of 200 W (2.0 A at 50  $\Omega$ ). The generator has an impedance feedback loop that maximizes energy delivery by minimizing charring. A peristaltic pump (model PE-PM; Valleylab) circulates chilled sterile water (approximately 18°–20°C at the electrode tips) through the electrodes. The single electrodes are 17 gauge (1.5 mm) in diameter, and, with the exception of a 3.0-cm-long exposed tip, the shaft is insulated. Each cluster electrode consists of three single electrodes set 5.0 mm apart in a triangular configuration. Each electrode in the cluster configuration is identical to a single electrode, with the exception of a 2.5-cm-long exposed tip.

In group 1—the single-electrode control ablations—and group 2—the cluster-electrode control ablations—coagulation zones were created at both 12 and 16 minutes. Twelve minutes is the accepted clinical-standard duration for single-electrode liver ablation with the Cool-tip system, and longer ablation times are not associated with larger co-

agulation volumes (21). A second, longer ablation duration, 16 minutes, was chosen because of the uncertainty as to whether longer multiple-electrode ablations could create larger coagulation zones.

**Multiple-electrode RF ablation.**—All of the multiple-electrode RF ablations (group 3) described in our study were performed by one author (P.F.L.) by using a prototype system based on the switching between three electrodes (22). In this system, the RF generator output was delivered to the electrodes through a personal computer-controlled electronic switch (Fig 1). Three single RF electrodes—each with a 3-cm active tip and each identical to the single electrode used in the control group—were placed 2.0 cm apart in an equilateral triangular configuration by using a template to ensure parallel placement. The interelectrode spacing of 2.0 cm was optimized in preliminary pilot experiments, in which spacing the electrodes 2.5 cm or more apart resulted in cleft, nonconglomerate coagulation zones. The impedance at each electrode was relayed to the personal computer, which controlled the electronic switch.

Power was switched from one electrode to the next when the impedance spiked—that is, reached 30  $\Omega$  above the baseline level (Fig 2). If the amount of time an electrode was off decreased to less than 5 seconds—owing to high impedance levels at all three electrodes—power was diverted to a 150- $\Omega$  resistive load for the remainder of the 5 seconds to allow the impedance of the tissue to decrease. As we did with the control ablations, we performed half the multiple-electrode ablations by applying power for 12 minutes and half by applying power for 16 minutes.

### Coagulation Zone Volume and Diameter Measurements

One author (P.F.L.) performed the coagulation zone measurements and analyses. The lengths of the coagulation zones were measured by using calipers, and then the zones were sliced axially at 3–4-mm intervals. The liver slices were placed directly onto an optical scanner (Perfection 2450 Photograph Model G860A; Epson, Long Beach, Calif), and electronic images of them were saved. The sizes of the coagulated regions were analyzed by using the freeware ImageJ

Figure 1

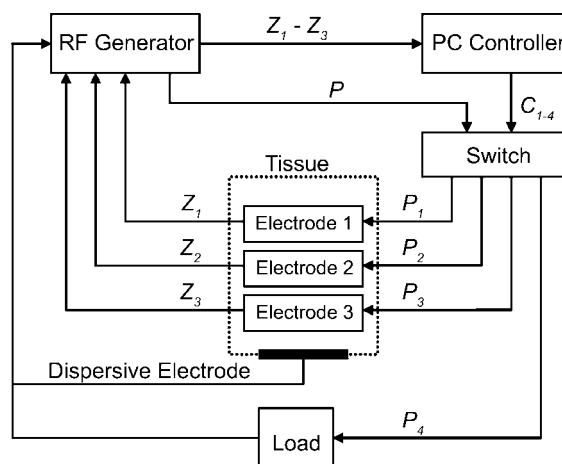


**Figure 1:** Diagram of multiple-electrode RF system. The impedances ( $Z_1$ – $Z_3$ ) of each of the three electrodes are reported to the RF generator, which relays the values to a personal computer (PC). The power ( $P$ ) is relayed to the electrode and the 150- $\Omega$  resistive load via the electronic switch. The signal ( $C_{1-4}$ ) determines which electrode the power is relayed to or if the power is relayed to the load. If the cycles of power application occur too rapidly or the impedance values of the three electrodes are too high, the power is diverted to the load for a predetermined amount of time.  $P_1$ – $P_3$  = power of each of three electrodes,  $P_4$  = power of resistive load.

(National Institute of Mental Health, Bethesda, Md). Measurements were taken in the central white zone of complete coagulation—not the surrounding red zone shown to contain viable cells (23–26). The volumes of coagulation were calculated by using the formula for the volume of an ellipsoid:  $(4/3)\pi abc$ , where  $a$ ,  $b$ , and  $c$  are the length axis

radius, width axis radius, and height axis radius, respectively. The length, minimum diameter, and maximum diameter, respectively, were used in place of these values in our study.

### Shape of Coagulation Zone

One author (P.F.L.) estimated the shape of the coagulation zone by calcu-

lating the mean isoperimetric ratio for each ablation group by using a representative liver slice, which was the same slice that was used to measure the minimum and maximum coagulation zone diameters. This ratio is an estimation of the roundness of the ablated region in two dimensions (25,27). The closer this ratio is to 1.0, the more round the zone of coagulation. The isoperimetric ratio (IR) was computed by using the equation  $IR = (4\pi \cdot A)/P^2$ , with the area ( $A$ ) and perimeter ( $P$ ) measured on the same section on which the minimum and maximum diameters were measured.

### Statistical Analyses

The single-, cluster-, and multiple-electrode RF ablation results were compared in terms of the sizes and shapes of the resulting coagulation zones. Analysis of variance was used to test for overall differences in mean isoperimetric ratio and mean minimum diameter, maximum diameter, length, and volume of coagulation across the different ablation techniques. Two-sample  $t$  tests were used to perform pairwise comparisons of each measurement between the ablation groups and to check for differences between the 12- and 16-minute durations within the groups. Bonferroni correction was used because of the large number of tests performed (five measurements performed three times each, for total of 15 tests). Therefore, statistical significance (with use of a standard cutoff of  $P < .05$ ) was based on an  $\alpha$  value of .0033 ( $0.05/15$ ).  $P$  values of between .05 and .0033 were considered to be suggestive of statistical significance.

## Results

### Comparison of Extent of Coagulation

At both 12 and 16 minutes of multiple-electrode RF ablation, we created coagulation zones with significantly larger mean diameters and volumes compared with those created with single-electrode RF ablation ( $P < .0033$ , analysis of variance and pairwise  $t$  tests) (Tables 1, 2; Figs 3–6). The mean minimum diame-

Figure 2

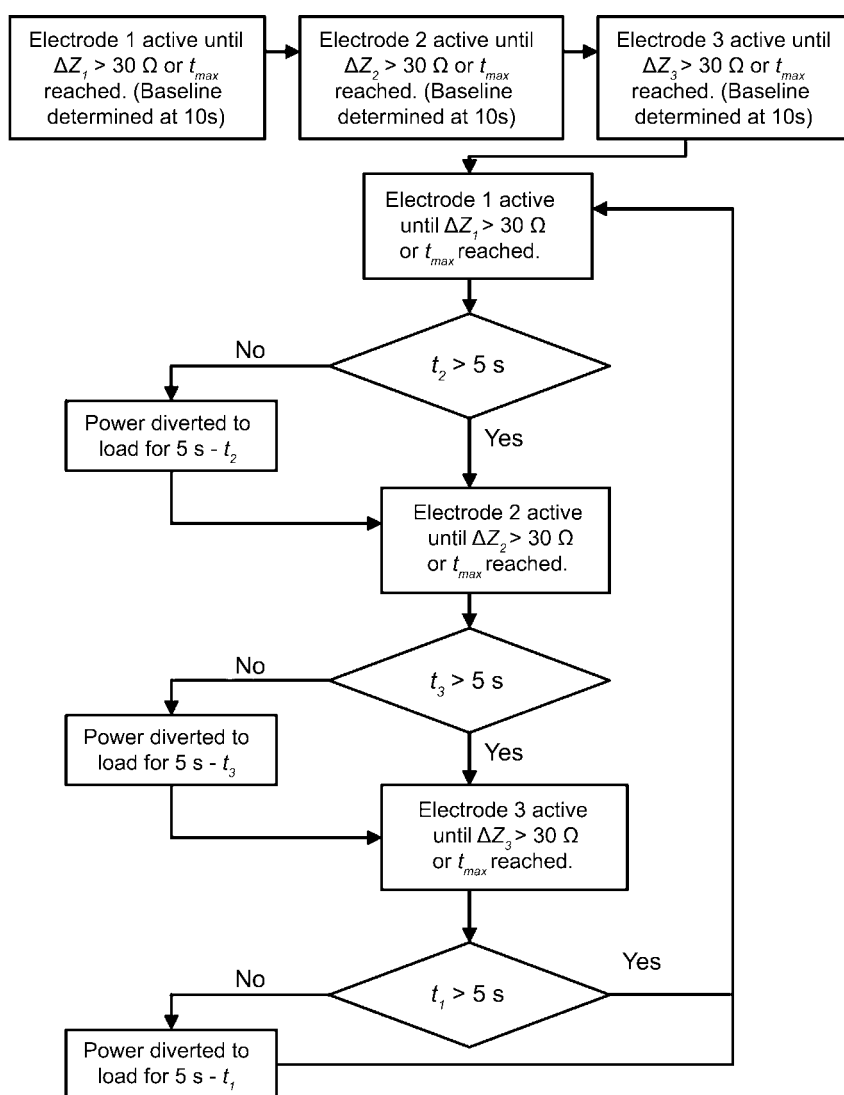


**Figure 2:** Diagram of impedance-switching algorithm. The algorithm involves activating each electrode sequentially until its impedance level reaches  $30\ \Omega$  above the baseline level or a maximum time interval ( $t_{max}$ ) is reached. A minimum time interval of 5 seconds is set as the amount of time that each electrode must be off. If the cycles of power application occur too rapidly, the power is diverted to the  $150\text{-}\Omega$  resistive load for the remainder of the 5-second interval.  $\Delta Z_1 - \Delta Z_3 =$  rise in impedance above baseline level for each of three electrodes,  $t_1 - t_3 =$  amount of time each of three electrodes has been off.

Table 1

## RF Ablation–induced Coagulation Zone Dimensions and Volume at 12 Minutes

Parameter	No. of Ablations	Minimum Diameter (cm)	Maximum Diameter (cm)	Length (cm)	Volume (cm <sup>3</sup> )	Isoperimetric Ratio
<b>Ablation</b>						
Single electrode	9	1.6 ± 0.6*	2.0 ± 0.5 <sup>††</sup>	3.6 ± 0.3	6.7 ± 3.7 <sup>§  </sup>	0.78 ± 0.15
Cluster electrode	6	2.1 ± 0.5	2.9 ± 0.3 <sup>†#</sup>	3.8 ± 0.2	12.7 ± 5.2 <sup>§</sup>	0.77 ± 0.11
Multiple electrode	6	2.8 ± 0.6*	4.2 ± 0.7 <sup>†#</sup>	3.4 ± 0.5	22.1 ± 10.7 <sup>  </sup>	0.71 ± 0.22
ANOVA <i>P</i> value <sup>**</sup>	NA	.006	<.0001	.20	.002	.75

Note.—Unless otherwise specified, values are means ± standard deviations.

\* *P* = .003 for difference between values obtained at single- versus multiple-electrode RF ablation.

† *P* = .001 for difference between values obtained at single- versus cluster-electrode RF ablation.

†† *P* < .0001 for difference between values obtained at single- versus multiple-electrode RF ablation.

§ *P* = .021 for difference between values obtained at single- versus cluster-electrode RF ablation.

|| *P* = .001 for difference between values obtained at single- versus multiple-electrode RF ablation.

# *P* = .02 for difference between values obtained at cluster- versus multiple-electrode RF ablation.

\*\* *P* values for overall differences in mean isoperimetric ratio and mean values of minimum diameter, maximum diameter, length, and volume of coagulation across the different ablation techniques, as calculated at analysis of variance (ANOVA). NA = not applicable.

Table 2

## RF Ablation–induced Coagulation Zone Dimensions and Volume at 16 Minutes

Parameter	No. of Ablations	Minimum Diameter (cm)	Maximum Diameter (cm)	Length (cm)	Volume (cm <sup>3</sup> )	Isoperimetric Ratio
<b>Ablation</b>						
Single electrode	9	1.7 ± 0.5 <sup>*†</sup>	2.2 ± 0.6 <sup>§§</sup>	3.6 ± 0.8	7.1 ± 3.5 <sup>§§</sup>	0.92 ± 0.05 <sup>§</sup>
Cluster electrode	6	2.3 ± 0.3 <sup>  </sup>	3.2 ± 0.4 <sup>†#</sup>	3.4 ± 0.4 <sup>**</sup>	13.1 ± 3.0 <sup>†††</sup>	0.88 ± 0.04 <sup>††</sup>
Multiple electrode	6	3.2 ± 0.6 <sup>†  </sup>	4.2 ± 0.6 <sup>§§</sup>	4.1 ± 0.2 <sup>**</sup>	29.1 ± 8.3 <sup>§††</sup>	0.66 ± 0.09 <sup>§§††</sup>
ANOVA <i>P</i> value <sup>§§</sup>	NA	<.0001	<.0001	.16	<.0001	<.0001

Note.—Unless otherwise specified, values are means ± standard deviations.

\* *P* = .036 for difference between values obtained at single- versus cluster-electrode RF ablation.

† *P* = .0001 for difference between values obtained at single- versus multiple-electrode RF ablation.

†† *P* = .004 for difference between values obtained at single- versus cluster-electrode RF ablation.

§ *P* < .0001 for difference between values obtained at single- versus multiple-electrode RF ablation.

|| *P* = .007 for difference between values obtained at cluster- versus multiple-electrode RF ablation.

# *P* = .005 for difference between values obtained at cluster- versus multiple-electrode RF ablation.

\*\* *P* = .006 for difference between values obtained at cluster- versus multiple-electrode RF ablation.

††† *P* = .001 for difference between values obtained at cluster- versus multiple-electrode RF ablation.

†††† *P* = .0003 for difference between values obtained at cluster- versus multiple-electrode RF ablation.

§§ *P* values for overall differences in mean isoperimetric ratio and mean values of minimum diameter, maximum diameter, length, and volume of coagulation across the different ablation techniques, as calculated at analysis of variance (ANOVA). NA = not applicable.

ter, maximum diameter, and volume of the coagulation zones created with multiple-electrode ablation were significantly larger than those created with cluster-electrode ablation at 16 minutes, but only the maximum diameter was significantly larger at 12 minutes (*P* = .02 for maximum diameter at 12 minutes, *P* = .007 for minimum diameter at 16 minutes, *P* = .005 for maxi-

mum diameter at 16 minutes, *P* = .001 for volume at 16 minutes; analysis of variance and pairwise *t* tests). No significant differences between the 12- and 16-minute ablation durations in terms of the size of the induced coagulation were seen within the groups, with the exception of increased mean length in the multiple-electrode group (3.4 cm ± 0.5 [standard deviation] at 12 minutes

vs 4.1 cm ± 0.2 at 16 minutes, *P* = .015).

### Shape of Coagulation Zone

The isoperimetric ratios achieved in the multiple-electrode ablation group were lower than those achieved in the control groups, partly because the three electrodes were placed in a triangular configuration (Tables 1, 2; Figs 7, 8). The

differences were not significant at 12 minutes. However, the mean multiple-electrode isoperimetric ratio was significantly lower compared with both the mean cluster- and the mean single-electrode

ratios at 16 minutes ( $P < .0033$  for both comparisons). This difference was due in part to the increased isoperimetric ratio with both single- and cluster-

electrode ablation when the duration was increased from 12 to 16 minutes ( $P = .017$  and  $.039$ , respectively).

**Figure 3**

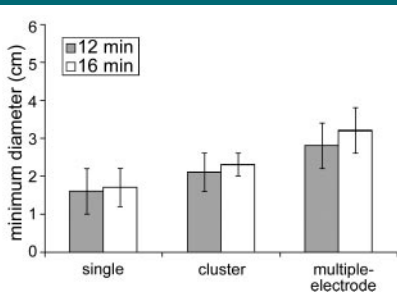


**Figure 3:** Graph illustrates mean minimum diameters for each of three ablation groups. Differences in values between the single- and multiple-electrode ablations were significant at both 12 and 16 minutes with use of uncorrected (.05) and corrected (.0033) cutoff  $P$  values. Differences in values between the single- and cluster-electrode ablations and between the cluster- and multiple-electrode ablations were significant at 16 minutes with use of uncorrected cutoff  $P$  value (.05). Error bars indicate standard deviations.

**Figure 4**

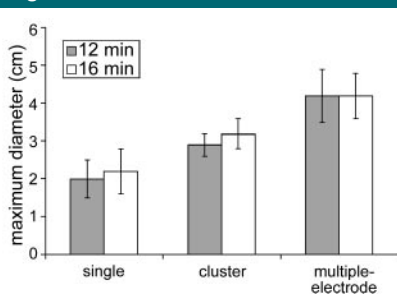


**Figure 4:** Graph illustrates mean maximum diameters for each of three ablation groups. Differences in values between the single- and multiple-electrode ablations were significant at 12 and 16 minutes with use of uncorrected (.05) and corrected (.0033) cutoff  $P$  values. Differences in values between the single- and cluster-electrode ablations were significant at 12 minutes. With use of the conservative uncorrected cutoff  $P$  value (.05), differences in maximum diameter among all three ablation groups were significant at both time points. No significant differences between the 12- and 16-minute ablation durations were seen within the groups. Error bars indicate standard deviations.

**Figure 5**

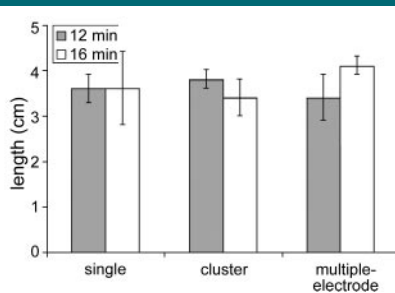


**Figure 5:** Graph illustrates mean lengths of induced coagulation in each of three ablation groups. The difference in mean length between the cluster- and multiple-electrode ablations at 16 minutes was significant ( $P = .006$ ). Furthermore, the lengths of the multiple-electrode-induced coagulation zones were significantly larger at 16 minutes than at 12 minutes ( $P = .015$ ). Some variation in length was expected, given that the active electrodes in the single- and multiple-electrode groups had a 3.0-cm-long tip, while those in the cluster-electrode group had a 2.5-cm-long tip. Error bars indicate standard deviations.

**Figure 6**

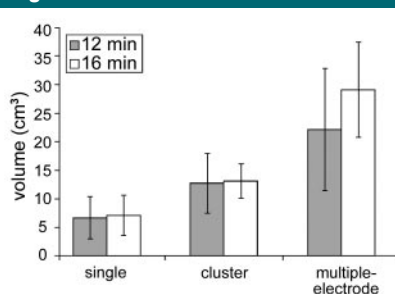


**Figure 6:** Graph illustrates mean volumes of induced coagulation in each of three ablation groups. Differences in mean volume between the multiple- and single-electrode ablations at both 12 and 16 minutes and between the multiple- and cluster-electrode ablations at 16 minutes were significant with use of both cutoff  $P$  values (.05 and .0033). The difference in mean volume between the cluster- and single-electrode ablations was significant only at 16 minutes with use of the conservative uncorrected cutoff  $P$  value (.05). Differences between the 12- and 16-minute ablation durations within the groups were not significant. Error bars indicate standard deviations.

## Discussion

RF ablation has been limited by the inability to create a coagulation zone large enough to consistently envelop the targeted tumor plus a 1.0-cm ablative margin. To treat a spherical tumor larger than 1.0 cm, a coagulation zone with a minimum diameter of greater than 3.0 cm is necessary. Reports of coagulation zones much larger than 3.0 cm—created primarily by using multiple-prong electrodes combined with saline infusion—have been published (28). However, many reports of large coagulation zones do not indicate the minimum diameter or the shape of the zone, and the absence of these data is a limiting factor when determining the effectiveness of a particular ablation procedure. Furthermore, high local recurrence rates for large tumors—particularly treated hepatic colorectal metastases—suggest that the current time-consuming strategy of consecutive overlapping ablations with single electrodes is not optimal.

**Figure 7**

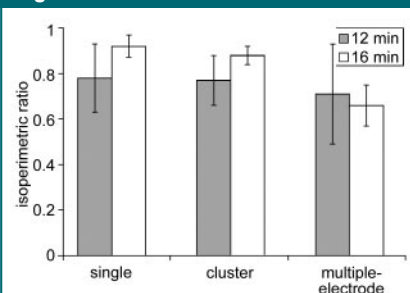


**Figure 7:** Graph illustrates mean isoperimetric ratios for coagulation zones in each of three ablation groups. The mean isoperimetric ratio achieved with multiple-electrode ablation at 16 minutes was significantly smaller than the ratios achieved with the cluster-electrode ( $P = .0003$ ) and single-electrode ( $P < .0001$ ) ablations. This difference was due in part to the significant increase in isoperimetric ratio achieved with both single-electrode ( $P = .017$ ) and cluster-electrode ( $P = .039$ ) ablation when the treatment time was increased from 12 to 16 minutes. Error bars indicate standard deviations.

Figure 8

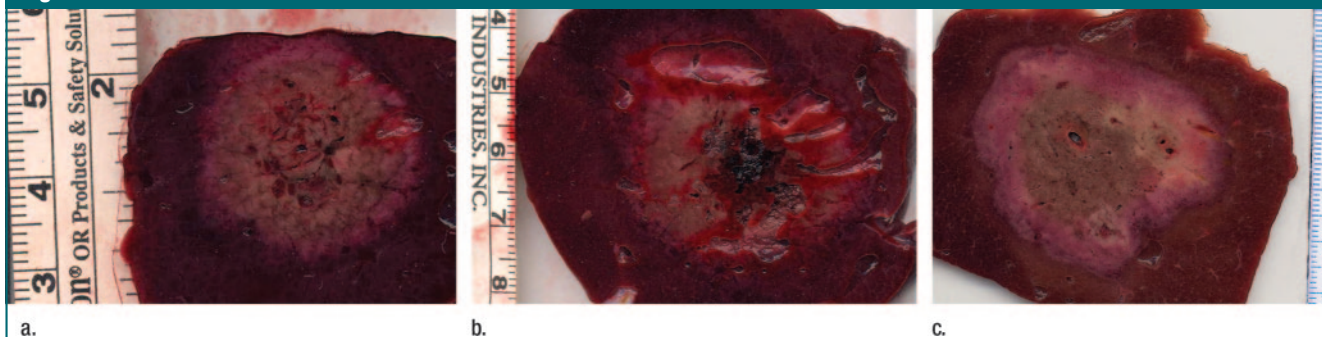


**Figure 8:** (a) Coagulation zone 2.0 cm in minimum diameter and 2.1 cm in maximum diameter created with single RF electrode. (b) Coagulation zone 2.8 cm in minimum diameter and 3.6 cm in maximum diameter created with cluster RF electrode. (c) Coagulation zone 4.0 cm in minimum diameter and 4.7 cm in maximum diameter created with multiple RF electrodes. In the multiple-electrode system, three electrodes were set in an equilateral triangular configuration and spaced 2.0 cm apart. A template was used to ensure proper interelectrode spacing at the electrode tips.

Therefore, more effective means of generating large coagulation volumes are needed.

In our study, the multiple-electrode system created volumes of coagulation that were 74% ( $22.1 \text{ cm}^3/12.7 \text{ cm}^3$ ) and 122% ( $29.1 \text{ cm}^3/13.1 \text{ cm}^3$ ) larger than the volumes created with cluster-electrode ablation at 12 and 16 minutes, respectively. The multiple-electrode ablation volumes also surpassed the predicted volume increase (three times the volume) when the three single electrodes were used simultaneously (3.3 and 4.1 times the single-electrode volumes at 12 and 16 minutes, respectively), in one-third of the time. These disproportionate volume increases infer that thermal synergy was achieved. To our knowledge, our study is the first with findings that demonstrate the capability of a multiple-electrode RF system to induce thermal synergy in an *in vivo* environment.

The phenomenon of thermal synergy is exclusive to multiple-applicator ablation systems. This effect has been demonstrated with both microwave ablation and cryoablation, where three simultaneously activated applicators created a conglomerate zone of coagulation with a volume larger than three times the volume achieved with single-applicator ablation (19,29). We believe that the thermal synergy achieved with multiple-electrode RF ablation has several mechanisms: First, the application of RF energy results in progressive vascu-

lar thrombosis and devascularization of the hepatic parenchyma. Therefore, activation of the first electrode helps to decrease the perfusion-mediated cooling of the two remaining electrodes. Activation of the second electrode decreases the perfusion-mediated cooling of the other two electrodes, and so forth. This process results in the rapid development of a large conglomerate zone of coagulation (25,30).

Second, unlike with sequential ablation, with multiple-electrode ablation, higher temperatures are achieved and maintained between the simultaneously heated electrodes because tissue heating occurs much faster than tissue cooling (13). Finally, with multiple-electrode ablation, the thermal boundary conditions are altered such that less energy is required to heat the periphery of each ablation zone because it becomes heated at above  $37^\circ\text{C}$  as the adjacent zone of ablation is created.

The development of multiple-electrode RF systems has been hindered by the electrical interactions that occur between simultaneously activated, closely spaced electrodes (11,13). An electric current flows between areas of high voltage (ie, the electrode) and areas of low voltage (ie, the ground pad). When multiple electrodes from the same power source are placed in close proximity, a weak current flows between the electrodes because they are at the same voltage (12). This factor fundamentally limits the distance at which the elec-

trodes can be separated owing to cool spots in the center of the ablation; this observation was made by Goldberg et al (31) during the development of the cluster electrode. Commercially available multiple-prong devices are limited by the weak current flow between electrode prongs. Attempting to increase the ablation zone size by setting the prongs further apart would cause increased irregularity in the shape of the induced coagulation, which is already a problem with these electrodes (32).

The multiple-electrode device assessed in our study enables the use of three electrically independent electrodes and obviates electrical interactions between them because only one electrode is powered at a time. Therefore, the electrodes generate heat in all directions and can be placed further apart than the electrodes currently installed in commercially available RF systems (13). In effect, the system simultaneously creates multiple overlapping ablation zones without the need for consecutive repositioning of a single electrode, which can be complicated by microbubbles, edema, and hemorrhage from earlier ablations. The system operates by switching to a different electrode at each impedance spike ( $>30 \Omega$  above baseline), because sharp increases in impedance are associated with tissue coagulation and vascular thrombosis, two desirable end points in the creation of a conglomerate zone of coagulation (33,34). Instead of tempo-

rarily switching the system off when an impedance spike is encountered, the generator powers a second electrode until an impedance spike and then powers the third electrode, and so on.

Switching electrodes at fixed time intervals is less efficient than using an impedance-controlled algorithm. For example, switching the electrode at a time shorter than that required to cause an impedance spike may lead to inadequate vascular thrombosis and thus allow intact perfusion to cool the tissue close to this electrode while other electrodes are activated. This tissue would have to be reheated during the next cycle of power application. Longer time intervals may be more effective in creating vascular thrombosis. However, after the impedance spikes, only minimal power can be delivered, and, thus, the time during which no electrodes are delivering power increases.

Spacing of electrodes 2.0 cm apart was chosen to maximize the extent of induced coagulation without compromising its shape. Pilot experience revealed that spacing electrodes 2.5 cm or more apart resulted in cleaving at the periphery of the coagulation zone. This greater spacing may increase the overall volume of coagulation, but it also increases the risk of creating irregularly shaped coagulation zones. To increase the space between electrodes and still create a conglomerate zone of coagulation, the power deposition would need to be increased by either using a high-power RF generator or lowering the impedance. Although these modifications are being actively pursued by our team and others, they were beyond the scope of our current study. Finally, our intention in this nontumor model was to create spherical coagulation zones. Ultimately, the best shape may not be exactly spherical and probably will need to be tailored on a case-by-case basis. For instance, electrode placement may be skewed to one side to minimize the heat sink effect of a vessel. We believe that electrodes could be placed to conform to the shape of the tumor in clinical settings.

Our study had limitations: First, all of the RF ablations were performed in normal, highly vascular pig livers. A large-animal tumor model would have

served as a better model, but we are unaware of any such animal models with tumors or organs large enough for the volume of tissue ablated in our study. Also, the right and left medial lobes of pig livers are the largest of the four lobes, and the associated hepatic and portal veins are very large. For the purposes of our study, multiple-electrode ablations were performed in these medial lobes because the large size of the resulting coagulation zone would have overwhelmed the lateral lobes. Consequently, the multiple-electrode coagulation zones possibly were smaller than those that would have been created if we had been able to distribute the ablations more evenly throughout the liver. Therefore, we possibly were conservative in our claims based on our study findings, as we would expect to create larger coagulation zones in the tumors of humans, which are less vascular.

The open surgical model used for our study was designed to maximize the number of ablations per animal and ultimately decrease the number of animals sacrificed. However, further investigation of the multiple-electrode system in a percutaneous environment is needed. It may be more difficult to place the electrodes in a percutaneous setting, especially when an intercostal approach is used. While our results indicate that optimal results are achieved when the electrodes are spaced 2 cm or less apart, the electrodes do not have to be placed exactly parallel and more than one intercostal space may be used.

**Practical application:** Our study results demonstrate the capability of a switched-multiple-electrode RF device to facilitate thermal synergy and create large areas of coagulation in an in vivo porcine liver model. In further studies, the use of techniques that increase the power delivered to tissue may yield even larger coagulation zones. Large-volume ablation performed with multiple-electrode systems may increase the effectiveness of RF ablation for treatment of larger tumors by enabling more consistent destruction of the entire tumor and a surrounding margin.

**Acknowledgments:** The authors gratefully acknowledge the efforts of Brandon Gay, Kyle R. Rick, and Steve Buysse in developing and testing the prototype multiple-electrode RF system.

## References

- Rosenthal DI, Hornicek FJ, Torriani M, Gebhardt MC, Mankin HJ. Osteoid osteoma: percutaneous treatment with radiofrequency energy. *Radiology* 2003;229:171-175.
- Lencioni RA, Allgaier HP, Cioni D, et al. Small hepatocellular carcinoma in cirrhosis: randomized comparison of radio-frequency thermal ablation versus percutaneous ethanol injection. *Radiology* 2003;228:235-240.
- Akeboshi M, Yamakado K, Nakatsuka A, et al. Percutaneous radiofrequency ablation of lung neoplasms: initial therapeutic response. *J Vasc Interv Radiol* 2004;15:463-470.
- Hwang JJ, Walther MM, Pautler SE, et al. Radio frequency ablation of small renal tumors: intermediate results. *J Urol* 2004;171:1814-1818.
- Cady B, Jenkins RL, Steele GD Jr, et al. Surgical margin in hepatic resection for colorectal metastasis: a critical and improvable determinant of outcome. *Ann Surg* 1998;227:566-571.
- Elias D, Cavalcanti A, Sabourin JC, et al. Resection of liver metastases from colorectal cancer: the real impact of the surgical margin. *Eur J Surg Oncol* 1998;24:174-179.
- Livraghi T, Goldberg SN, Lazzaroni S, Meloni F, Solbiati L, Gazelle GS. Small hepatocellular carcinoma: treatment with radiofrequency ablation versus ethanol injection. *Radiology* 1999;210:655-661.
- Kosari K, Gomes M, Hunter D, Hess DJ, Greeno E, Sielaff TD. Local, intrahepatic, and systemic recurrence patterns after radiofrequency ablation of hepatic malignancies. *J Gastrointest Surg* 2002;6:255-263.
- Kuvshinoff BW, Ota DM. Radiofrequency ablation of liver tumors: influence of technique and tumor size. *Surgery* 2002;132:605-611.
- Machi J, Uchida S, Sumida K, et al. Ultrasound-guided radiofrequency thermal ablation of liver tumors: percutaneous, laparoscopic, and open surgical approaches. *J Gastrointest Surg* 2001;5:477-489.
- Halliday D, Resnick R, Walker J. *Fundamentals of physics*. New York, NY: Wiley, 2000.
- Haemmerich D, Tungjitkusolmun S, Staelin ST, Lee FT Jr, Mahvi DM, Webster JG. Finite-element analysis of hepatic multiple probe radio-frequency ablation. *IEEE Trans Biomed Eng* 2002;49:836-842.

13. Haemmerich D, Lee FT Jr, Schutt DJ, et al. Large-volume radiofrequency ablation of ex vivo bovine liver with multiple cooled cluster electrodes. *Radiology* 2005;234:563–568.
14. Dodd GD 3rd, Frank MS, Aribandi M, Chopra S, Chintapalli KN. Radiofrequency thermal ablation: computer analysis of the size of the thermal injury created by overlapping ablations. *AJR Am J Roentgenol* 2001;177:777–782.
15. Lencioni R, Cioni D, Bartolozzi C. Percutaneous radiofrequency thermal ablation of liver malignancies: techniques, indications, imaging findings, and clinical results. *Abdom Imaging* 2001;26:345–360.
16. Varghese T, Techavipoo U, Zagzebski JA, Lee FT Jr. Impact of gas bubbles generated during interstitial ablation on elastographic depiction of in vitro thermal lesions. *J Ultrasound Med* 2004;23:535–544.
17. Mitchell CK, Smoger SH, Pfeifer MP, et al. Multivariate analysis of factors associated with postoperative pulmonary complications following general elective surgery. *Arch Surg* 1998;133:194–198.
18. Singh B, Cordeiro PG, Santamaria E, Shaha AR, Pfister DG, Shah JP. Factors associated with complications in microvascular reconstruction of head and neck defects. *Plast Reconstr Surg* 1999;103:403–411.
19. Wright AS, Lee FT Jr, Mahvi DM. Hepatic microwave ablation with multiple antennae results in synergistically larger zones of coagulation necrosis. *Ann Surg Oncol* 2003;10:275–283.
20. Institute of Laboratory Animal Research, Commission on Life Sciences, National Research Council. Guide for the care and use of laboratory animals. Washington, DC: National Academy Press, 1996.
21. Goldberg SN, Solbiati L, Hahn PF, et al. Large-volume tissue ablation with radio frequency by using a clustered, internally cooled electrode technique: laboratory and clinical experience in liver metastases. *Radiology* 1998;209:371–379.
22. Lee FT Jr, Haemmerich D, Wright AS, Mahvi DM, Sampson LA, Webster JG. Multiple probe radiofrequency ablation: pilot study in an animal model. *J Vasc Interv Radiol* 2003;14:1437–1442.
23. Ng KK, Lam CM, Poon RT, et al. Porcine liver: morphologic characteristics and cell viability at experimental radiofrequency ablation with internally cooled electrodes. *Radiology* 2005;235:478–486.
24. Goldberg SN, Gazelle GS, Compton CC, Mueller PR, Tanabe KK. Treatment of intrahepatic malignancy with radiofrequency ablation: radiologic-pathologic correlation. *Cancer* 2000;88:2452–2463.
25. Chinn SB, Lee FT Jr, Kennedy GD, et al. Effect of vascular occlusion on radiofrequency ablation of the liver: results in a porcine model. *AJR Am J Roentgenol* 2001;176:789–795.
26. Cha CH, Lee FT Jr, Gurney JM, et al. CT versus sonography for monitoring radiofrequency ablation in a porcine liver. *AJR Am J Roentgenol* 2000;175:705–711.
27. Do Carmo MP. Differential geometry of curves and surfaces. Englewood, NJ: Prentice-Hall, 1976.
28. Miao Y, Ni Y, Yu J, Zhang H, Baert A, Marchal G. An ex vivo study on radiofrequency tissue ablation: increased lesion size by using an “expandable-wet” electrode. *Eur Radiol* 2001;11:1841–1847.
29. Rewcastle JC, Sandison GA, Muldrew K, Saliken JC, Donnelly BJ. A model for the time dependent three-dimensional thermal distribution within iceballs surrounding multiple cryoprobes. *Med Phys* 2001;28:1125–1137.
30. Chang I, Mikityansky I, Wray-Cahen D, Pritchard WF, Karanian JW, Wood BJ. Effects of perfusion on radiofrequency ablation in swine kidneys. *Radiology* 2004;231:500–505.
31. Goldberg SN, Gazelle GS, Dawson SL, Rittman WJ, Mueller PR, Rosenthal DI. Tissue ablation with radiofrequency using multiprobe arrays. *Acad Radiol* 1995;2:670–674.
32. Pereira PL, Trubenbach J, Schenk M, et al. Radiofrequency ablation: in vivo comparison of four commercially available devices in pig livers. *Radiology* 2004;232:482–490.
33. Arata MA, Nisenbaum HL, Clark TW, Soulen MC. Percutaneous radiofrequency ablation of liver tumors with the LeVeen probe: is roll-off predictive of response? *J Vasc Interv Radiol* 2001;12:455–458.
34. Berber E, Herceg NL, Casto KJ, Siperstein AE. Laparoscopic radiofrequency ablation of hepatic tumors: prospective clinical evaluation of ablation size comparing two treatment algorithms. *Surg Endosc* 2004;18:390–396.